ELSEVIER

Catalysis Today 78 (2003) 181–190

CATALYSIS TODAY

www.elsevier.com/locate/cattod

Preparation and characterisation of vanadium catalysts supported over alumina-pillared clays

M.A. Vicente [a,*], C. Belver [a], R. Trujillano [a], M.A. Bañares-Muñoz [a], V. Rives [a], S.A. Korili [b], A. Gil [b], L.M. Gandía [b], J.-F. Lambert [c]

[a] *Departamento de Química Inorgánica, Universidad de Salamanca, Plaza de la Merced s/n, E-37008 Salamanca, Spain*
[b] *Departamento de Química Aplicada, Edificio Los Acebos, Universidad Pública de Navarra, Campus de Arrosadía s/n, E-31006 Pamplona, Spain*
[c] *Laboratoire de Reactivité de Surface, Université Pierre et Marie Curie, 4 Place Jussieu, Tour 54, Casier 178, 75252 ParisCedex 05, France*

Abstract

Supported vanadium-containing catalysts were prepared by impregnation of Al-pillared clays with $NaVO_3$ precursor aqueous solutions. A montmorillonite and a saponite, both natural as well as previously pillared with Al_{13}-Keggin polycations, were used as supports, being impregnated with solutions of the precursor by means of the incipient wetness technique. The layered structure of the supports is maintained after impregnation, and even after calcination of the impregnated solids at 500 °C, although with a significant worsening of the textural properties of the solids, in particular, a loss of specific surface area. Three crystalline vanadium-containing phases were identified in the impregnated solids, namely, NaV_3O_8, $AlVO_4$ and V_2O_5 (shcherbinaite). The reduction of these phases to V^{3+} species was observed as wide processes in the 450–750 °C range, all of them centred at ca. 600 °C.

Keywords: Al-pillared clays; Supported vanadium catalysts; Saponite; Montmorillonite

1. Introduction

Impregnation with precursors of catalytically active phases constitutes a classical method to prepare heterogeneous catalysts. Usually, precursors of transition metals are deposited on the supports by means of ionic exchange or incipient wetness or dry impregnation, the solids most widely used as supports being alumina, silica, titania, zirconia or zeolites [1]. The use of clays, both natural or chemically modified by different methods (acid activation, thermal activation, pillaring) has received less attention [2].

Pillared interlayered clays (PILCs), form a well-known family of microporous materials prepared by multi-step molecular engineering processes (the literature on pillared clays has been very extensive in the last years, two recent review articles in this field are: [3]). First, the interlayer cations of a layered swellable clay are exchanged by bulk inorganic polyoxocations, leading to the intercalated clays. In the second step, the intercalated clays are calcined at a moderate temperature, the polyoxocations being transformed into pillars, thus leading to the pillared solids. This step is carried out due to the poor thermal stability of the intercalated clays, which

* Corresponding author. Tel.: +34-923-294489; fax: +34-923-294574.
E-mail address: mavicente@usal.es (M.A. Vicente).

0920-5861/02/$ – see front matter
PII: S0920-5861(02)00328-0

may be considered as intermediate precursors of the final stable pillared clays. Therefore, pillared clays may be viewed as clay layers separated by metallic oxide-based pillars, which avoid their collapse, or alternatively, as dispersed nanometric oxide particles which aggregation is hindered by the presence of the clay layers. Accordingly, these solids may be considered nanocomposite materials, where two different components are intermingled at the molecular scale.

The presence of large porosity and high specific surface area, together with the possibility of controlling the textural properties of the pillared solids by changing the clay nature (montmorillonite, saponite, hectorite, etc.), the intercalating species nature (polycations based on Al^{3+}, Si^{4+}, Ti^{4+}, Zr^{4+}, Cr^{3+}, Fe^{3+} or Ga^{3+}, etc.), the concentration of intercalating species, etc., give to these solids interesting properties as catalysts, catalyst supports and adsorbents [3]. However, the use of pillared clays as supports for the preparation of catalysts has received a limited attention. This is in part due to the relatively large and complicated synthesis procedure, which justifies the use of these solids only for very specific reactions. Nevertheless, catalysts based on Al- or Zr-pillared montmorillonites or saponites impregnated with Pt, Rh, Pd, Cu, Cr, Fe, Mo or Ni salts have been prepared [3 and references therein], and in some cases tested in catalysed reactions, such as hydroxylation of phenol to dihydroxybenzenes, selective catalytic reduction (SCR) of NO, hydroisomerisation of alkanes, hydrocracking of octane, hydroformylation of ethylene and propene, propene metathesis, complete oxidation of volatile organic compounds (VOCs), etc.

A few papers describing the preparation of V/pillared clay catalysts can be found in the literature. Bahranowski et al. [4–8] have studied the nature of the V species on low-loaded $VOSO_4$ on Al-, Ti- and Zr-pillared montmorillonite catalysts. The catalytic performance of the solids for the oxidative dehydrogenation of propane, ammoxidation of *m*-xylene and SCR of NO by ammonia was also investigated. Occelli et al. [9] have reported the impregnation of Al-pillared rectorite with vanadyl naphthenate, and studied the evolution of the samples by EDS, HREM and ^{51}V solid-state MAS NMR, finding a preferential location of V in the micropores of the impregnated solids, but collapsing under calcination. Khedher and Ghorbel [10] have reported the use of a V/montmorillonite catalyst, prepared by impregnation of an acid-treated montmorillonite with $VOCl_3$, in the reaction of epoxidation of allylic alcohol.

In the present paper, we report on the preparation of V/clay catalysts, prepared by impregnation of both the natural and Al-pillared forms of a montmorillonite and a saponite with aqueous $NaVO_3$ solutions. The impregnated solids have been characterised by means of elemental–chemical analyses, X-ray diffraction, thermal analyses, UV-Vis-NIR spectroscopies, TPR and N_2 adsorption measurements.

2. Experimental

2.1. Raw materials, Al-PILCs synthesis and catalysts preparation

Two natural smectite clays were selected as starting materials, namely, a saponite from Ballarat, CA, USA (Clay Minerals Repository, University of Missouri, DC, USA), and a montmorillonite from Gador, Almería, Spain (Minas de Gador, S.L.). These clays were purified by careful aqueous dispersion and decantation, and the fractions with particle size smaller than 2 μm were submitted to intercalation with aluminium polycations. Some data of the starting clays are given here, and further details of their characterisation can be found elsewhere [11].

Ballarat saponite. Chemical composition of the fraction with particle size lesser than 2 μm (weight percentage, wt.%)—SiO_2: 47.83; Al_2O_3: 4.46; Fe_2O_3: 0.98; MgO: 26.75; TiO_2: 0.07; MnO: 0.02; CaO: 0.80; Na_2O: 0.24; K_2O: 0.14; and loss by ignition: 18.7 wt.%. Cation exchange capacity: 0.90 meq/g. Basal spacing: 14.1 Å. Specific Langmuir surface area: 37 m^2/g.

Gador montmorillonite. Chemical composition of the fraction with particle size lesser than 2 μm (wt.%)—SiO_2: 54.00; Al_2O_3: 20.71; Fe_2O_3: 2.21; MgO: 4.33; TiO_2: 0.15; MnO: 0.08; CaO: 1.09; Na_2O: 0.21; K_2O: 0.12; and loss by ignition: 17.1 wt.%. Cation exchange capacity: 1.17 meq/g. Basal spacing: 15.4 Å. Specific Langmuir surface area: 140 m^2/g.

Al-pillared clays were prepared by means of the following synthetic procedure. The Al-polycations, namely $[Al_{13}O_4(OH)_{24}(H_2O)_{12}]^{7+}$, were prepared by slow titration of a solution of $AlCl_3{\cdot}6H_2O$ (Panreac,

PA) with a 1 M NaOH (Panreac, 97%) solution, under vigorous stirring and using an OH^-/Al^{3+} molar ratio of 2.2. The hydrolysed solution was aged for 24 h at room temperature under constant agitation (pH = 4.1). This solution was added to previously prepared suspensions (1 wt.%) of the purified clays in deionised water, using a ratio of 5 mmol Al per gram of clay. The new suspensions were stirred for 24 h at room temperature and then centrifuged and washed by dialysis with distilled water until no chloride (Ag^+ test) was detected in the washing liquids. The resulting intercalated clays were dried in air at 50 °C for 16 h and then calcined in air at 500 °C for 4 h (heating rate 1 °C/min). These solids are designated as BAsap-Al and GAmont-Al for Al-pillared Ballarat saponite and Gador montmorillonite, respectively.

Supported vanadium catalysts were prepared by incipient wetness impregnation of the above described supports with aqueous $NaVO_3$ (Sigma-Aldrich, tech., 90%) solutions, in order to obtain a content of ca. 10 wt.% V_2O_5 in the final solids. In order to impregnate 2 g of a pillared clay, 0.27 g $NaVO_3$ were dissolved in about 3 cm^3 of water, which were dropwise added to the solid up to incipient wetness was reached. Then, the solid was dried at 100 °C and the impregnation process repeated, the process being completed after 3 cycles. The solids were then dried, and calcined at 500 °C. The solids are designated as V/BAsap-Al(100) and V/GAmont-Al(100) for the solids only dried at 100 °C, and V/BAsap-Al(500) and V/GAmont-Al(500) for those calcined at 500 °C.

Two additional vanadium catalysts were prepared using the natural clays as supports (2 μm fractions previously calcined at 500 °C). These solids are referred to as V/BAsap(100) and V/GAmont(100) for the samples only dried at 100 °C, and V/BAsap(500) and V/GAmont(500) for the ones calcined at 500 °C.

2.2. Characterisation techniques

X-ray powder diffraction patterns were obtained by using a Siemens D-500 diffractometer, operated at 40 kV and 30 mA (1200 W), with nickel-filtered Cu Kα radiation (λ = 1.54 Å). The equipment was connected to a DACO-MP microprocessor and used Diffract-AT software.

Elemental–chemical analyses of the solids were carried out by Activation Laboratories Ltd. (Ancaster, Ont., Canada), using inductively coupled plasma spectroscopy (ICPS) and atomic absorption spectroscopy (AAS).

Textural analyses were carried out from the corresponding nitrogen (Air Liquide, 99.999%) adsorption at −196 °C, obtained from a static volumetric apparatus (Micromeritics ASAP 2010 adsorption analyzer). The nitrogen adsorption data were collected in the relative pressure range 10^{-5}–0.99. To obtain an adequate characterisation of the microporous region, sufficient data points at low pressures are needed, and this requires the addition of constant small nitrogen volumes. The nitrogen adsorption data were obtained using about 0.2 g of sample and successive nitrogen doses of 4 cm^3/g until a relative pressure of 0.01 was reached. Each point of the adsorption isotherm in this range was equilibrated for at least 2 h. Further nitrogen was added and the volumes required to achieve a fixed set of relative pressures up to 0.99 were measured. Previous to analysis, samples were degassed at 200 °C for 24 h ($p < 10^{-3}$ mm Hg).

UV-Vis and NIR spectra were recorded in the region 190–2500 nm in the reflectance mode by using a Cary 5 spectrometer, with an optical length of 0.2 cm.

Temperature-programmed reduction (TPR) analyses were carried out by using a Micromeritics TPR/TPD 2900 instrument, at a heating rate of 10 °C/min, employing ca. 20 mg of sample and 60 cm^3/min of a 5 vol.% H_2/Ar mixture (Air Liquide) as reducing gas. Experimental conditions were chosen according to Malet and Caballero [12], in order to attain a good resolution of the reduction peaks. Hydrogen consumption was measured by a thermal conductivity detector (TCD). Water and other compounds that may be formed during cations reduction and sample decomposition were trapped using an isopropanol slurry to avoid interference with the measured signal.

Scanning electron microscopy (SEM) was performed using a Zeiss DSM 940 Digital Scanning Microscope, operating at 25 kV over samples in which a thin gold layer was deposited by evaporation using a Bio-Rad ES100 SEN coating system.

3. Results and discussion

Characterisation results showed that the supports properties accord with the ones usually found for both

Table 1
Basal spacing, fwhm index, and intensity of the $d(0\,0\,1)$ reflections for the natural, pillared and impregnated samples (the H_2/V molar ratios for the impregnated samples calcined at 500 °C are also given)

Sample	$d(0\,0\,1)$ (Å)	fwhm, 2θ (°)	Intensity (cps)	H_2/V ratio
Natural clays				
BAsap	14.1	1.004	2465	
GAmont	15.4	1.173	1532	
Supports				
BAsap(500)	10.9	1.528	1132	
BAsap-Al(500)	17.8	0.709	6151	
GAmont(500)	10.6	1.612	985	
GAmont-Al(500)	17.7	1.545	2503	
Supported catalysts				
V/BAsap(100)	12.5	1.106	2358	
V/BAsap(500)	12.4	1.666	1479	1.07
V/BAsap-Al(100)	18.1	1.035	4334	
V/BAsap-Al(500)	17.5	[b]	1437	0.90
V/GAmont(100)	10.0	1.360[a]	573	
V/GAmont(500)	10.0	1.141[a]	562	1.62
V/GAmont-Al(100)	18.0	1.126[a]	1260	
V/Gamont-Al(500)	18.0	[b]	914	1.28

[a] Very wide and weak intense peaks.
[b] Not measurable.

natural and pillared clays. The main characteristics of the natural clays have been given above. When calcined at 500 °C, the basal spacings decreased to 10.9 and 10.6 Å, and the specific surface areas to 27 and 130 m^2/g, respectively, for saponite and montmorillonite samples. On the other hand, the pillared solids showed well-ordered layered structures with basal spacings of 17.8 Å (saponite) and 17.7 Å (montmorillonite), and specific surface areas of 256 and 249 m^2/g, respectively (see Tables 1 and 2), which indicates that the pillaring process has been successful in both cases.

The chemical compositions of the impregnated solids are given in Table 3. All samples showed final V_2O_5 contents ranging from 7.18 to 8.41%, when referred to water-free, ignited solids, together with an increase of about 3.5% of the content of Na_2O, probably from the V precursor salt. The small differences among the V_2O_5 contents in the different samples, and also the deviation of these contents with respect to the expected 10 wt.% content, are due to the different hydration degree of the supports. For comparison, the chemical compositions of the natural and pillared clays, referred to water-free samples, are also included in Table 3. The differences between the natural and pillared clays are the ones usually due to the pillaring process, i.e., removal of the exchangeable cations of the clays (mainly Ca^{2+} in the case of montmorillonite and both Ca^{2+} and Na^{+} in the case of saponite), the fixation of Al from the polycations, and the subsequent small relative decrease in the content of the other metallic elements. No significant differences were observed between the impregnated samples and the corresponding supports other than the decrease in the relative content of other metallic elements due to the deposition of V and Na.

The solids obtained by impregnation and drying of the pillared clays showed basal spacings between 17 and 18 Å, which remained almost unchanged after calcination at 500 °C. All the samples showed the typical patterns of layered solids, however, ordering of the solids decreased considerably on impregnating: this effect is illustrated in Fig. 1 by comparing several XRD patterns, whereas in Table 1 the full widths at half maximum, fwhm indexes, of the solids are compared. The higher values of this index for the impregnated solids indicate a lower stacking ordering of the layers in the *c* direction as a result of catalyst preparation.

The solids prepared by impregnation of the natural clays showed basal spacings close to 12 Å (saponite) and 10 Å (montmorillonite), which remained almost unchanged after calcination at 500 °C. This fact may be the result of a strong, or even complete, collapse and disorganisation of the clays during the impregnation step. A basal spacing of 12 Å corresponds to saponite swelled by a sheet of water molecules: natural saponites are usually hydrated with two sheets of water molecules ($d_{0\,0\,1}$ = 14–14.5 Å) [13], but it should be considered that, in our case, the natural clay was previously calcined at 500 °C ($d_{0\,0\,1}$ = 10.9 Å). Thus, it may be reasonable that saponite layers are partially rehydrated during impregnation, remaining swelled by water to 12 Å. If so, the vanadium species might diffuse into the saponite interlayer spacing. In the case of the montmorillonite, such a rehydration is not observed, and the basal spacing, ca. 10 Å, corresponds to the tetrahedral–octahedral–tetrahedral (TOT) minimum spacing. Loss of ordering during the process (the 0 0 1 reflection in the XRD pattern of the final solids is absent) suggests the collapse and/or delamination of

Table 2
Textural properties derived from the nitrogen adsorption isotherms at 77 K of the samples indicated

Sample	A_{LANG} (m^2/g)[a]	A_{ext} (m^2/g)[b]	V_p (cm^3/g)[c]	HK		$\sum V_p$ (cm^3/g)[d]
				$V_{\mu p(HK)}$ (cm^3/g)[e]	$d_{p(HK)}$ (Å)[f]	
Natural clays						
BAsap	37 ($C = 196$)[g]	27	0.107	0.017	8.2	0.068
GAmont	140 ($C = 275$)	55	0.180	0.059	5.8; 8.1	0.113
Supports						
BAsap(500)	27 ($C = 196$)	23	0.106	0.012	8.7	0.069
BAsap-Al(500)	256 ($C = 308$)	33	0.183	0.096	5.4; 7.2	0.072
GAmont(500)	130 ($C = 279$)	62	0.191	0.054	6.1; 8.5	0.127
GAmont-Al(500)	249 ($C = 487$)	33	0.168	0.093	5.3; 6.7	0.063
Supported catalysts						
V/BAsap(500)	2 ($C = 328$)	1	0.011	0.001	–	0.006
V/BAsap-Al(500)	31 ($C = 307$)	4	0.039	0.012	8.9	0.017
V/GAmont(500)	18 ($C = 51$)	8	0.040	0.006	10.2	0.024
V/GAmont-Al(500)	65 ($C = 305$)	5	0.060	0.024	7.3	0.023

[a] Specific surface areas from the Langmuir equation ($0.01 \leq p/p^0 \leq 0.05$, interval of relative pressure).
[b] Specific external surface areas obtained from the *t*-method.
[c] Specific total pore volumes at $p/p^0 = 0.99$.
[d] Cumulative pore volumes from the BJH method (for pores in the range 17–500 Å).
[e] Specific micropore volumes derived from the HK method.
[f] Maxima of the HK micropore size distributions.
[g] Langmuir *C*-value, characteristic of the intensity of the adsorbate–adsorbent interactions.

the clay layers during the impregnation step. The 10 Å peak observed after calcination at 500 °C may also correspond to the very small amount of illite existing as an impurity in the natural clays, which diffraction lines are better observed upon the loss of intensity of the montmorillonite peaks. In brief, partial (saponite) or total (montmorillonite) collapse of the clay structure is the most probable one of these situations; dehydration is probably being favoured by the impregnation process, as natural saponites and montmorillonites are usually not completely dehydrated even when calcined at 500 °C. Thus, in the case of montmorillonite, the vanadium species may be mostly randomly located in the external part of the layers; although a small part of them might be located in the interlayer space, their concentration would not be large enough to produce an

Table 3
Chemical analyses (wt.%) of the supports and of the supported catalysts[a]

Sample	SiO_2	Al_2O_3	MgO	Fe_2O_3	MnO	TiO_2	CaO	Na_2O	K_2O	V_2O_5
Supports										
BAsap(500)	58.84	5.49	32.90	1.21	0.02	0.09	0.98	0.29	0.17	–
GAmont(500)	65.15	24.98	5.22	2.66	0.09	0.18	1.32	0.25	0.14	–
BAsap-Al(500)	55.51	14.21	27.75	1.16	0.02	0.20	0.77	0.02	0.35	–
GAmont-Al(500)	59.92	32.72	3.80	2.52	0.08	0.15	0.01	0.03	0.10	–
Supported catalysts										
V/BAsap(500)	52.94	4.79	27.76	1.02	0.02	0.20	1.26	4.38	0.49	7.18
V/BAsap-Al(500)	48.42	13.04	24.23	1.03	0.02	0.18	0.70	3.57	0.41	8.41
V/GAmont(500)	57.93	22.47	4.64	2.65	0.08	0.15	0.81	3.40	0.03	7.84
V/GAmont-Al(500)	53.05	29.89	3.41	2.14	0.05	0.14	0.12	3.56	0.08	7.57

[a] Results referenced to ignited solids (0% water).

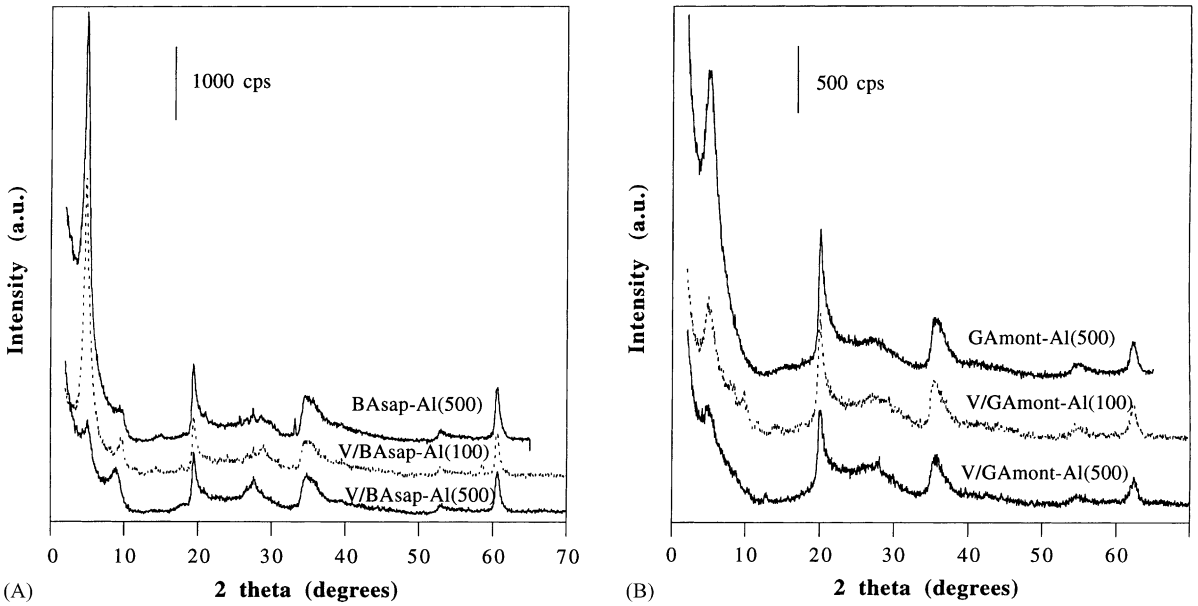

Fig. 1. XRD patterns of the samples corresponding to the series prepared from the pillared clays: (A) series from Ballarat saponite; (B) series from Gador montmorillonite.

XRD peak corresponding to an ordered pattern along the *c* axis.

The XRD patterns of the catalysts calcined at 500 °C showed very weak peaks of vanadium species. Up to three crystalline compounds could be identified in the different solids, namely, NaV_3O_8, $AlVO_4$ and V_2O_5 (shcherbinaite), while $NaVO_3$ was not detected in the calcined solids. As indicated, the peaks of the crystalline phases observed are very weak, suggesting the presence of rather small and disperse particles of the above-cited phases. The presence of dispersed, amorphous vanadium species cannot be ruled out as they would be undetectable by the experimental techniques here used. Formation of $AlVO_4$ requires the leaching of Al from the supports; although this process may be expected to be easier from the pillars than from the octahedral sheet of the clay, this phase was only clearly identified in the non-pillared V/BAsap(500) sample.

The UV-Vis-NIR spectra showed some differences between the dried precursors and the catalysts calcined at 500 °C (see Fig. 2, after standard Kubelka–Munk transformations). The main difference corresponds to the large intensities of the ca. 1380 and 1910 nm bands in the spectra of the dried solids, while two bands between 2200 and 2400 nm showed almost the same pattern for both the dried and the calcined solids. The band at 1380 nm can be assigned to the overtone of the OH stretching vibration, while the band at 1910 nm is due to the $(\nu + \delta)$ combination band of water, and the bands at 2200–2400 nm are due to the $(\nu + \delta)$ combination band of structural OHs. The trends observed when calcining the impregnated precursors are similar to that reported by Vicente and Lambert when calcining intercalated and Pt-impregnated clays [14], and is in accordance with the phenomena occurring when heating natural or treated clays at 500 °C, i.e., a significant loss of water molecules, but without removal of structural OH groups.

Some UV-Vis spectra are given in Fig. 3. All the spectra show a strong charge transfer band between the O ligands and the V central atom between ca. 190–400 nm, with 3–4 weak peaks in this region, located at ca. 200, 230, 280 and 315 nm, very similar for all four solids considered. Other effects are observed at higher wavelengths, which are different between the dried and the calcined solids. In the case of V/BAsap(100), small shoulders are observed at 439, 503 and 645 nm, whereas for V/BAsap(500) two shoulders were observed at 514 and 650 nm. The effects at 439 and 503 nm can also be assigned to

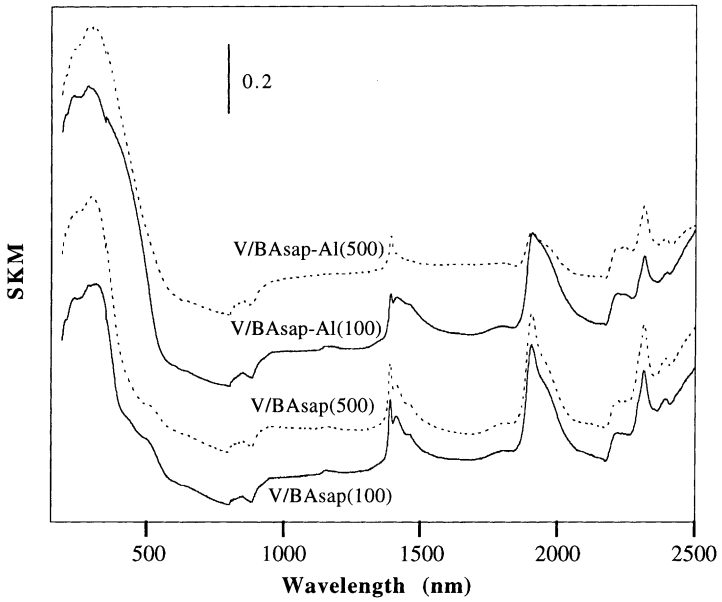

Fig. 2. UV-Vis-NIR spectra of dried and calcined V-impregnated solids derived from Ballarat saponite.

O → V charge transfer processes, the change in their form suggesting a modification in the dispersion of vanadium, but it should be noticed that the band at ca. 635 nm has been attributed to V(IV) d–d transitions [10], thus suggesting a partial reduction of the V(V) species, confirmed by the disapparition of these band when calcining the solids at 500 °C. In the case of the solids prepared from the pillared clays, the 190–400 nm region is similar, but the bands due to the support dominate the region of higher wavelengths.

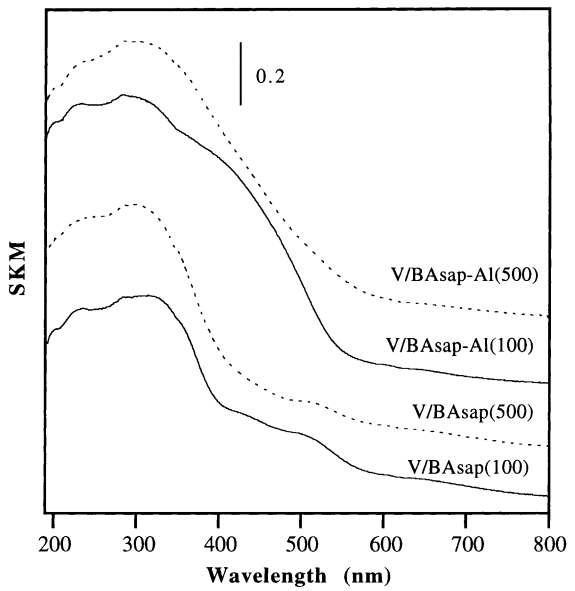

Fig. 3. Detailed UV-Vis spectra of dried and calcined V-impregnated solids derived from Ballarat saponite.

The reduction behaviour of the vanadium catalysts was studied by means of TPR; reduction curves of representative samples are showed in Fig. 4. Under the experimental conditions used, only $V^{5+} \rightarrow V^{3+}$ reduction processes are expected. In all cases, reduction of the vanadium species can be observed as a strong effect beginning at about 450 °C and centred at ca. 600 °C. This is a broad effect for the solids prepared from the natural clays, whereas it is sharper for the solids prepared from pillared clays, suggesting an easier access of hydrogen to the vanadium species when using the pillared clays as supports, or a broader distribution of vanadium in several reducible species when using the natural clays. This would accord with the fact that the reduction temperatures are lower for V/BAsap-Al(500) than for V/BAsap(500). The TPR profile of this last sample shows a reduction peak that begins at about 500 °C, reaches a maximum at 627 °C, and exhibits a shoulder at higher temperature (689 °C). In all cases, a small reduction effect can be observed

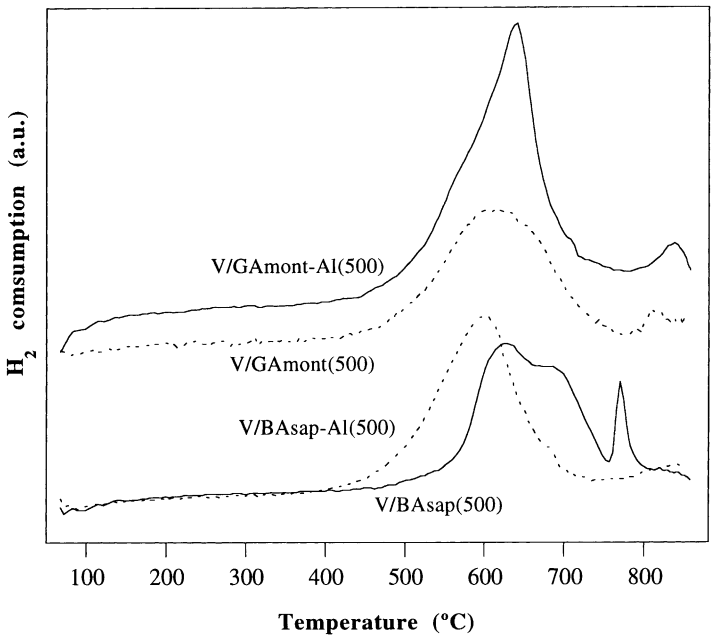

Fig. 4. TPR curves for the V-impregnated catalysts. Patterns have been vertically displaced for clarity.

at about 800 °C, which can be assigned to the reduction of the octahedral cations of the clays, mainly Fe^{3+} [15]. In the case of the V/BAsap(500) catalyst, a very sharp effect is observed at 768 °C which is absent in the TPR profile of the V/BAsap-Al(500) sample. The molar ratio between the amount of H_2 consumed in the reduction process and the V present in the solids is included in Table 1. In the case of the solids prepared from saponite, this ratio is close to 1, suggesting a reduction process from V(V) to V(III). However, this ratio increases in the solids prepared from montmorillonite, reaching a value as high as 1.62 for the V/GAmont(500) catalyst. For these samples, a significant effect of the octahedral clay Fe^{3+} cations may be proposed. The Fe_2O_3 content in the montmorillonite is relatively high, more than twice the content of this oxide in the saponite. Considering that the reduction of Fe^{3+} consumes 1.5 times more hydrogen than that of V^{5+} (Fe^{3+} can be reduced to the zero-valent state, $Fe^{3+} \rightarrow Fe^0$), the amount of hydrogen that could be consumed by the Fe^{3+} present in the montmorillonite is almost equivalent to that consumed by 8 wt.% V_2O_5. So, the clay composition has to be taken into account when analysing the TPR results. Nevertheless, although with some differences between the various samples, the $V^{5+} \rightarrow V^{3+}$ reduction process may be proposed as the one that predominates in all cases.

The textural properties of the samples are more explicitly given in Table 2. The intercalation with aluminium polycations caused a notable increase of the specific surface areas (A_{Lang}) and both the total (V_p) and the microporous specific pore volumes ($V_{\mu p(HK)}$) with respect to the natural clay. The natural clays were characterised by relatively high specific total surface areas and specific pore volumes, which is particularly true for Gador montmorillonite. Calcination at 500 °C decreased by 7–27% the specific surface areas, indicating a significant thermal stability. The alumina-pillared clays exhibit remarkable specific surface areas, reaching values as high as 256 m^2/g for BAsap-Al(500) and 249 m^2/g for GAmont-Al(500), thus multiplying by a factor between 1.9 and 9.5 the specific surface area of the unpillared clays. A more detailed description of the microporous and mesoporous regions of the clays has been obtained from the pore size distributions obtained from the Horvath–Kawazoe (HK) [16] and

Barrett–Joyner–Halenda (BJH) [17] methods. The specific microporous volumes, calculated according to the method proposed by Gil and Grange [18], and the maxima of the distributions for all clays, are also included in Table 2. The microporous volumes of the pillared clays are remarkably higher than that of the calcined unpillared clays. The pore size distributions of the supports show bimodal patterns, while the ones of the supported solids have monomodal patterns. Bimodal distribution in pillared clays has been related to bimodal micropore sizes as well as to the presence of two main types of adsorption surfaces on micropores, the position of the maxima being related to the pillar density in the interlayer region [19,20]. Thus, the change from bimodal to monomodal distribution during impregnation may be related to the blocking of part of the micropore region by the vanadium species. The cumulative mesopore volumes ($\sum V$p) of the samples for pores in the range between 17 and 500 Å, as determined by the BJH analysis, are also given in Table 2. The mesoporous size range is not influenced by the intercalation or the calcination processes. Only Gador montmorillonite shows a decrease of the specific external surface area (A_{ext}) and the mesoporous volume upon intercalation. This behaviour has been related in the literature to various factors [20].

When comparing the nitrogen adsorption of the clay support and of the supported vanadium oxide catalysts, it can be noticed that both the micropores and mesopores of the supports seem to be strongly affected by the presence of vanadium species, which produces important modifications in the specific surface area and specific pore volume values. A decrease of textural properties after impregnation of pillared clays with metal-precursors because of the blocking of the interlayer and interpillar spacings of the solids has been previously reported [15,21,22].

The study of the textural properties of the solids was completed by means of SEM. Some micrographs of the supports and of the dried and calcined impregnated solids, in the saponite series, are shown in Fig. 5. It can be observed that the presence of vanadium species produces solids less spongy than before the impregnation, suggesting that the change in the form of the particles can contribute to the

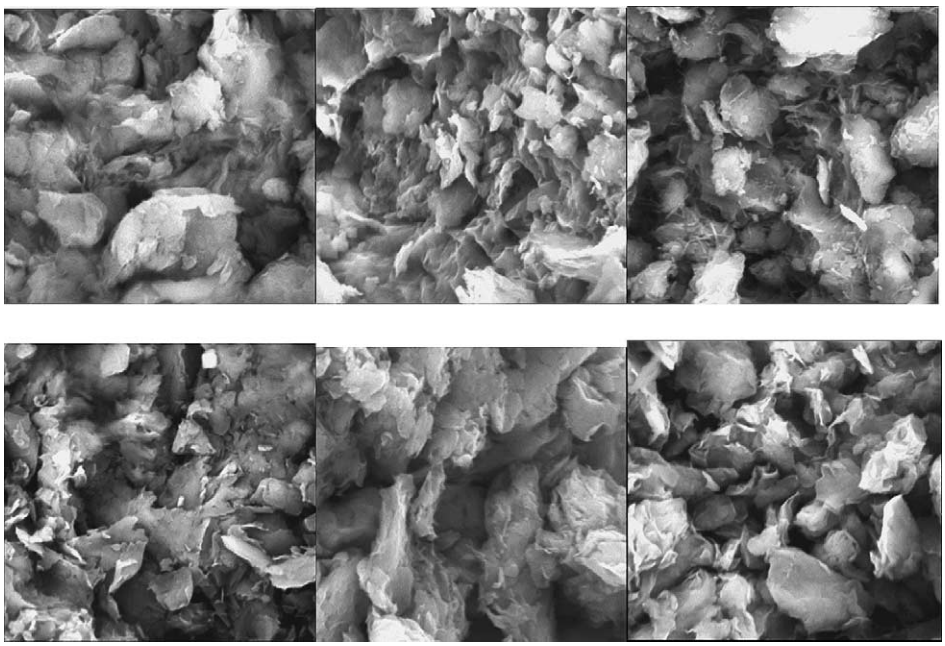

Fig. 5. SEM micrographs of the support (left), and of the dried (centre) and calcined (right) V-impregnated solids prepared from natural (up) and pillared (down) Ballarat saponite. Amplification is 5000 for all micrographs.

worsening of the textural properties. Thus, an aggregation of the particles seems to occur, where the V_2O_5 crystallites may act as nuclei for such an aggregation.

4. Conclusions

Various supported vanadium catalysts have been prepared by impregnating with aqueous solutions of $NaVO_3$ two clays, a saponite and a montmorillonite, both in their natural and Al-pillared forms. The impregnation preserved the layered structure of the supports, but with a strong decrease in the specific surface area and in the specific pore volume of the solids. Disperse NaV_3O_8, $AlVO_4$ and V_2O_5 (shcherbinaite) were the vanadium species detected in the impregnated solids upon calcination at 500 °C. These phases were reduced by hydrogen to the V(III) state species by means of wide processes in the 450–750 °C range. No significant differences were found when comparing the saponite- and the montmorillonite-based catalysts. The catalytic behaviour of these samples would merit to be investigated.

Acknowledgements

This work has been developed in the frame of a Spain-France bilateral collaboration project (Spanish Ministry of Science and Technology, MCyT, Acción Integrada HF2000-0106 and Ministère des Affaires Étrangères, Action Intégrée Programme Picasso No. 02630 TE). MABM, MAV and CB also thank the financial support from MCyT (MAT1999-0956). CB acknowledges a predoctoral Grant from MCyT, Formación de Personal Investigador (FPI) Program (PN-05424782).

References

[1] G. Ertl, H. Knözinger, J. Weitkamp (Eds.), Preparation of Solid Catalysts, Wiley/VCH, Weinheim, 1999.
[2] R.S. Varma, Tetrahedron 58 (2002) 1235.
[3] (a) A. Gil, L.M. Gandía, M.A. Vicente, Catal. Rev. Sci. Eng. 42 (2000) 145;
(b) Z. Ding, J.T. Kloprogge, R.L. Frost, G.Q. Lu, H.Y. Zhu, J. Porous Mater. 8 (2001) 273.
[4] K. Bahranowski, E.M. Serwicka, Geol. Carpath. Clays 44 (1993) 17.
[5] K. Bahranowski, E.M. Serwicka, Colloid Surf. A 72 (1993) 153.
[6] K. Bahranowski, R. Dula, J. Komorek, T. Romotowski, E.M. Serwicka, Stud. Surf. Sci. Catal. 91 (1995) 747.
[7] K. Bahranowski, M. Labanowska, E.M. Serwicka, Appl. Magn. Reson. 10 (1996) 477.
[8] K. Bahranowski, J. Janas, T. Machej, E.M. Serwicka, L.A. Vartikian, Clay Miner. 32 (1997) 665.
[9] M.L. Occelli, J.M. Dominguez, H. Eckert, J. Catal. 141 (1993) 510.
[10] I. Khedher, A. Ghorbel, Stud. Surf. Sci. Catal. 130 (2000) 1649.
[11] (a) R. Toranzo, Ph.D. Thesis, Universidad de Salamanca, 2001;
(b) R. Toranzo, M.A. Vicente, M.A. Bañares-Muñoz, L.M. Gandía, A. Gil, Micropor. Mesopor. Mater. 24 (1998) 173.
[12] P. Malet, A. Caballero, J. Chem. Soc., Faraday Trans. I 84 (1988) 2369.
[13] H. Suquet, J.T. Iiyama, H. Kodama, H. Pezerat, Clays Clay Miner. 25 (1977) 231.
[14] M.A. Vicente, J.-F. Lambert, Phys. Chem. Chem. Phys. 1 (1999) 1633.
[15] L.M. Gandía, A. Gil, M.A. Vicente, Appl. Catal. A 196 (2000) 281.
[16] G. Horvath, K. Kawazoe, J. Chem. Eng. Jpn. 16 (1983) 470.
[17] G.P. Barrett, L.G. Joyner, R.H. Halenda, J. Am. Chem. Soc. 73 (1951) 373.
[18] A. Gil, P. Grange, Langmuir 13 (1997) 4483.
[19] R.T. Yang, M.S.A. Baksh, AIChE J. 37 (1991) 679.
[20] A. Gil, M.A. Vicente, L.M. Gandía, Micropor. Mesopor. Mater. 34 (2000) 115.
[21] A. Gil, M.A. Vicente, J.-F. Lambert, L.M. Gandía, Catal. Today 68 (2001) 41.
[22] M.A. Vicente, J.F. Lambert, Phys. Chem. Chem. Phys. 3 (2001) 4843.